hunchback is required for suppression of abdominal identity, and for proper germband growth and segmentation in the intermediate germband insect *Oncopeltus fasciatus*

Paul Z. Liu and Thomas C. Kaufman*

Howard Hughes Medical Institute, Department of Biology, Indiana University, 1001 East Third Street, Bloomington IN, 47405, USA
*Author for correspondence (e-mail: kaufman@bio.indiana.edu)

Accepted 18 December 2003

Development 131, 1515-1527
Published by The Company of Biologists 2004
doi:10.1242/dev.01046

Summary

Insects such as *Drosophila melanogaster* undergo a derived form of segmentation termed long germband segmentation. In long germband insects, all of the body regions are specified by the blastoderm stage. Thus, the entire body plan is proportionally represented on the blastoderm. This is in contrast to short and intermediate germband insects where only the most anterior body regions are specified by the blastoderm stage. Posterior segments are specified later in embryogenesis during a period of germband elongation. Although we know much about *Drosophila* segmentation, we still know very little about how the blastoderm of short and intermediate germband insects is allocated into only the anterior segments, and how the remaining posterior segments are produced. In order to gain insight into this type of embryogenesis, we have investigated the expression and function of the homolog of the *Drosophila* gap gene *hunchback* in an intermediate germ insect, the milkweed bug, *Oncopeltus fasciatus*. We find that *Oncopeltus hunchback* (*Of'hb*) is expressed in two phases, first in a gap-like domain in the blastoderm and later in the posterior growth zone during germband elongation. In order to determine the genetic function of *Of'hb*, we have developed a method of parental RNAi in the milkweed bug. Using this technique, we find that *Oncopeltus hunchback* has two roles in anterior-posterior axis specification. First, *Of'hb* is required to suppress abdominal identity in the gnathal and thoracic regions. Subsequently, it is then required for proper germband growth and segmentation. In milkweed bug embryos depleted for *hunchback*, these two effects result in animals in which a relatively normal head is followed by several segments with abdominal identity. This phenotype is reminiscent to that found in *Drosophila hunchback* mutants, but in *Oncopeltus* is generated through the combination of the two separate defects.

Key words: *hunchback*, *hb*, Short germband, Segmentation, *Oncopeltus*, Growth zone, RNAi, Parental RNAi

Introduction

Though all insects possess a highly conserved adult body plan, this morphological conservation belies an underlying developmental diversity that gives rise to this body plan. For example, insects are described as being 'short', 'intermediate' or 'long' germband and show fundamental differences in how their body segments are generated (Davis and Patel, 2002; Krause, 1939; Sander et al., 1985). Long germband segmentation is evolutionarily derived and in this form of embryogenesis, all body segments are specified early and simultaneously during the blastoderm stage. As short and intermediate germ segmentation is found throughout the insects, whereas the long germ type is restricted to the higher insects, it is likely that a form of short or intermediate germband segmentation is evolutionarily ancestral (Davis and Patel, 2002). In this mode of segmentation, only the anterior-most segments are specified during the blastoderm stage, leaving the rest of the body plan to be specified later in embryogenesis, during germband elongation. (Because the short and intermediate forms of segmentation are conceptually so similar, for convenience sake we will refer to both the short and intermediate forms as 'short'.)

The fruitfly, *Drosophila melanogaster* exhibits long germband segmentation. In this fly, embryogenesis begins with the first nuclear divisions occurring without concomitant cellular divisions. Then nuclei fated to form the blastoderm migrate to the egg periphery and persist as a syncytium before cellularization. During the blastoderm stage, action of the segmentation gene cascade serves to subdivide this blastoderm into smaller and smaller regions, producing all the body segments (reviewed by St Johnston and Nüsslein-Volhard, 1992). By the end of the blastoderm stage, fate maps show that all of the future body regions including the head, thorax and the entire abdomen are already represented proportionally on the *Drosophila* blastoderm (Lohs-Schardin et al., 1979).

This is in contrast to short germband segmentation. In this type of segmentation, nuclei fated to contribute to the embryo proper migrate to the egg cortex and cellularize, as in *Drosophila*. However, it is during the blastoderm phase where the differences between short and long germband segmentation become apparent. In short germband segmentation, only anterior segments – typically the head and thoracic regions – are proportionally represented upon the blastoderm fate map.

It is only after the formation of the germband and during germband growth that the rest of the body forms. The posterior segments arise from a disproportionately small region of the posterior of the germ anlagen, termed the 'growth zone'. This 'growth zone' has not yet been well characterized but is the posterior-most region of the proliferating germband. Growth of this region results in germband elongation during which the rest of the segments are specified. Thus, although long germ segmentation can be thought of as successive spatial subdivision of the early blastoderm, short germ segmentation entails both spatial and temporal aspects, spatial during the blastoderm phase with the temporal aspect occurring later during germband elongation (reviewed by Davis and Patel, 2002).

How is the blastoderm of short germband insects patterned to yield only the anterior-most segments? How does the 'growth zone' generate the posterior segments and how are these segments specified? Moreover, how did long germband segmentation evolve from the short form? Although much has been learned about the genetics that regulate long germband segmentation from *Drosophila*, we unfortunately know little about short germ segmentation. Our understanding of *Drosophila* segmentation can provide clues, but not answers to these questions. Therefore in order to gain insight into how the evolution from short to long occurred, and to get a better picture of insect segmentation in general, we must address our lack of understanding of short germband segmentation.

The striking embryological differences between short and long germ segmentation imply fundamental differences in patterning at the molecular level. For this reason, the roles of a few early developmental genes involved in anteroposterior axis specification have been the focus for understanding these differences. In *Drosophila*, the gap genes are responsible for the early subdivision of the blastoderm into broad regions, each of which will eventually encompass several adjacent body segments. As one of the essential differences between short and long germ segmentation lies in the early allocation of the blastoderm fate map, it seems reasonable to compare the action of the gap genes in short and long germ insects. We focus our attention on the gap gene *hunchback* (*hb*).

hunchback encodes a zinc-finger-containing transcription factor known to be important for axial patterning in a number of insects (Jürgens et al., 1984; Lehmann and Nüsslein-Volhard, 1987; Patel et al., 2001; Schröder, 2003; Tautz et al., 1987). *Drosophila* embryos mutant for *hunchback* show a gap phenotype, with deletions of the labial through third thoracic segments and the eighth abdominal segment.

We have investigated the role of *hunchback* in an intermediate germband insect, the milkweed bug, *Oncopeltus fasciatus* (Hemiptera:Lygaeidae). We first examined embryogenesis and segmental specification in this bug using *engrailed* staining. We then reported the expression pattern of *Oncopeltus hunchback* (*Of'hb*) during embryogenesis. A technique for parental RNAi has been previously reported for *Tribolium castaneum* (Bucher et al., 2002), and we have adapted this technique for use in milkweed bugs in order to determine the function of *Of'hb* in segmentation. We find that *Of'hb* is required both for suppressing abdominal identity in the gnathal and thoracic segments, and for proper growth and segmentation of the abdomen.

Materials and methods

Cloning

RNA was isolated from ovaries quickly dissected under cold Robb's Minimal Saline (Robb, 1969) and flash frozen in liquid nitrogen. Embryonic RNA was isolated from mixed stage embryos. Total RNA was extracted using Trizol (GibcoBRL/Life Technologies) and poly(A^+) RNA was isolated using the Oligotex mRNA minikit (Qiagen). cDNA was synthesized using the FirstChoice RLM-RACE kit (Ambion). All PCRs were performed using the Advantage2 polymerase mix (BD Biosciences/Clontech). For the degenerate *hunchback* PCR, the primer pair was: AARCACCAYY-TNGARTAYCA-GTGWGMRTAYTTRCKCARRTG. 5′ and 3′ RACE PCRs were performed using a gene-specific primer and the anchor primers supplied in the FirstChoice RLM-RACE kit. After separation on an agarose gel, candidate PCR products were gel extracted if necessary (Qiagen), and cloned using the PCR-Script Amp Cloning Kit (Stratagene). At least three independent PCRs were performed and several clones sequenced in order to minimize PCR and sequencing artifacts. The *Of'hb* sequence has been submitted to GenBank under Accession Number AY460341. The *Oncopeltus engrailed* 5′ RACE fragment used to make the *en* in situ probe was cloned by designing primers to the previously identified homeodomain region (Peterson et al., 1998) and the sequence has been submitted to GenBank under Accession Number: AY460340.

Northern analysis

Total RNA samples used in northern analysis were prepared as for cloning (see above). Probes for both northern analysis and in situ hybridization were synthesized from a 1.1 kb clone containing the 3′ end of the *Of'hb* ORF (Fig. 2C). Northern probes were prepared with biotin-UTP (Enzo) using the MAXIscript kit (Ambion). Northern blotting was performed using the NorthernMax kit (Ambion) onto BrightStar-Plus membrane (Ambion) and detected using the BrightStar BioDetect kit (Ambion).

Embryo and ovary fixation

The chorions on germband stage embryos were cracked by first shaking in 1:1 heptane:12% paraformaldehyde in PBTw for 20 minutes and then heptane/methanol cracked. After chorion cracking, embryos were fixed for 1 hour in 4% paraformaldehyde in PBT. For blastoderm preparation, it was necessary to first boil the eggs for 1 minute before continuing with the chorion cracking procedure. Ovaries for in situ hybridization were isolated by quick dissection in cold Robb's Minimal Saline, gently rocked in heptane for a few minutes, and fixed in 4% paraformaldehyde in PBTw for 1 hour.

In situ hybridization

In situ probes were prepared with digoxigenin-UTP, biotin-UTP or fluorescein-UTP (Roche) using the MAXIscript kit (Ambion). The in situ protocol used here was based largely on that of O'Neill and Bier (O'Neill and Bier, 1994) with some modifications. After embryos were fixed, they were soaked for 1 hour in RIPA detergent mix [150 mM NaCl, 1% NP-40, 0.5% sodium deoxycholate, 0.1% SDS, 1 mM EDTA, 50 mM EDTA, 50 mM Tris-HCl, pH 8.0]. Inclusion or omission of a proteinase K digestion step did not seem to affect the in situ results. In order to inactivate endogenous phosphatases, the embryos were incubated in hybridization buffer [50% formamide, 5× saline sodium citrate (SSC), 100 μg/ml heparin, 100 μg/ml sonicated calf thymus DNA, 100 μg/ml yeast RNA, 0.1% Tween-20] at 70°C for 30 minutes. Embryos were then pre-hybridized at 60°C for 30 minutes before hybridization with probe at 60°C for 36 hours. Embryos were washed several times and soaked overnight at 60°C in hybridization buffer. We found that short washes in lower-salt solutions, first [50% formamide, 5× SSC, 0.1% Tween-20], then in [50% formamide, 2× SSC, 0.1% Tween-20] helped reduce background. After washing several times in PBTw, embryos were

incubated in antibody hybridization solution [PBTw, 2 mg/ml bovine serum albumin (BSA), 5% normal sheep serum] for at least 1 hour. Alkaline phosphatase conjugated anti-digoxigenin, anti-biotin or anti-fluorescein antibody (Roche) was added to the embryos and allowed to rock overnight at 4°C. The next day, excess antibody was washed off in several changes in PBTw. The final color development step was carried out essentially as described Hauptmann and Gerster (Hauptmann and Gerster, 2000) except for two-color in situs where the first AP antibody was inactivated by heating to 70°C for 30 minutes followed by additional fixation for 2 hours before continuing with the second AP antibody.

RNAi

Template for the in vitro transcription reactions was prepared one of two ways. Plasmids containing the insert of interest were linearized by restriction digest, or template was prepared from a PCR where T3 and T7 phage promoter sequences were added to the primers. Sense and anti-sense RNA was synthesized in two separate reactions using the MEGAscript kit (Ambion). After purification, the sense and anti-sense RNAs were mixed to a final concentration of 2 μg/μl total RNA. The RNA was then annealed in injection buffer (Spradling and Rubin, 1982) by heating in a thermocycler to 94°C and held at this temperature for 3 minutes, then slowly cooled to 45°C over the course of 1 hour. Proper annealing of the RNA was confirmed on an agarose gel. Parts of the gene to which these dsRNAs were made are shown in Fig. 2C.

Embryonic RNAi injections were carried out as previously described (Hughes and Kaufman, 2000). For the parental RNAi injections, the dsRNA was loaded into a Hamilton #801 syringe with a 32 gauge point #2 needle. Virgin female *Oncopeltus* were anesthetized in CO_2 and injected in the abdomen between the fourth and fifth abdominal sternites with ~5 μl of dsRNA solution. This volume was necessarily variable due to wound leakage. Injected females were then reared individually with males and allowed to lay eggs. Eggs were allowed to develop at 25°C and were harvested 76-80 hours after egg lay for in situs, while embryos for morphological phenotypic analysis were allowed to develop fully.

Readers are encouraged to contact the authors directly for more detailed protocols.

Results

Oncopeltus embryology

A description of *Oncopeltus* embryogenesis using classical histological techniques has been reported previously (Butt, 1947). In order to orient the reader to bug embryogenesis, we augment this previous work with our own observations using a fluorescent nuclear dye and also with stainings for a segment polarity gene, *engrailed*.

Oncopeltus embryogenesis can be divided into two distinct phases – a blastoderm phase, which in some ways is similar to that of *Drosophila*, and a germband growth phase which it shares with other short germ insects. *Oncopeltus* embryogenesis begins with the first nuclear divisions occurring synchronously within the yolk mass without concomitant cellular divisions. After several such divisions, the resulting cleavage nuclei migrate to the egg cortex. By fifteen hours after egg lay, they reach the surface of the egg and after an additional two hours, the formation of cell membranes is complete (Fig. 1A) (Butt, 1947). At this stage, the large ovoid blastoderm superficially appears very *Drosophila* like. However, blastoderm cells of a 36- to 40-hour-old embryo are not evenly arranged around the yolk but are concentrated in two broad lateral domains on either side of the yolk mass (Fig. 1B) that are similar to the 'lateral plates' seen in *Rhodnius* (Butt, 1947; Mellanby, 1935).

In addition to observing the cellular movements in the blastoderm, we also wanted to ascertain the number of segments that have been specified at this stage in embryogenesis. As the segment polarity gene *engrailed* (*en*) is expressed in the posterior compartments of segments in many arthropods, including *Oncopeltus*, it serves as a convenient molecular segmental marker (Hughes and Kaufman, 2002; Patel et al., 1989; Rogers and Kaufman, 1996; Telford and Thomas, 1998). In situ hybridization of 36- to 40-hour-old embryos with *Oncopeltus engrailed* (*Of'en)* probe revealed a total of six vertical stripes on the blastoderm surface (Fig. 1C). This shows that by this stage, the blastoderm has already been allocated into six segments. We followed the migration of these stripes throughout embryogenesis to deduce their segmental affinities and have determined that these six initial stripes correspond to the mandibular through third thoracic segments. That *engrailed* is expressed at this stage is somewhat surprising, and shows that anterior patterning has occurred all the way to the segment polarity level long before the posterior body regions even exist. This reinforces the idea that although the *Oncopeltus* blastoderm may in some ways superficially resemble the *Drosophila* blastoderm, the milkweed bug blastoderm is subdivided in a distinctly different way.

Oncopeltus embryos are of the 'invaginating' type, which refers to the cell movements that give rise to the germband. Shortly after the formation of the blastoderm lateral plates, the germband begins to form when the cells at the posterior end of the blastoderm dive into the center of the yolk mass. The early site of invagination is marked by a small pit at the posterior pole of the late blastoderm (arrowheads in Fig. 1B,C). The cells of the blastoderm surface migrate towards the posterior, while the leading tip of the elongating germband dives into the interior of the yolk mass, towards the anterior pole of the egg. In order to visualize these movements, it is instructive to imagine the blastoderm as an inflated balloon, with invagination occurring as if a finger is poked into the interior of the balloon. Thus, the cells on the outside of the blastoderm move towards the posterior of the egg, dive into the yolk and migrate towards the anterior of the egg. This can easily be seen by comparing Fig. 1C, where six stripes of *engrailed* expressing cells lie on the blastoderm surface, to Fig. 1D1 and 1D2, where the invaginating germband has pulled the two posterior stripes into the yolk, leaving the four anterior stripes on the surface of the blastoderm. As germband invagination continues, the tip of the germband eventually reaches the anterior pole of the egg and the resulting germband stage embryo ends up with its head at the posterior of the egg (the embryo does eventually right itself through later embryonic movements). As these embryonic movements can potentially lead to confusion, when discussing the blastoderm we will refer to the anteroposterior and dorsoventral axis in regards to the fate maps of the tissues.

During the germband stage, the remaining posterior body segments that were not specified during blastoderm stage are now produced through elongation of the posterior portion of the germband coupled with progressive anterior to posterior segmental specification. First, the abdominal region is generated through rearrangement and growth of the posterior growth zone and then *engrailed* stripes appear one by one in

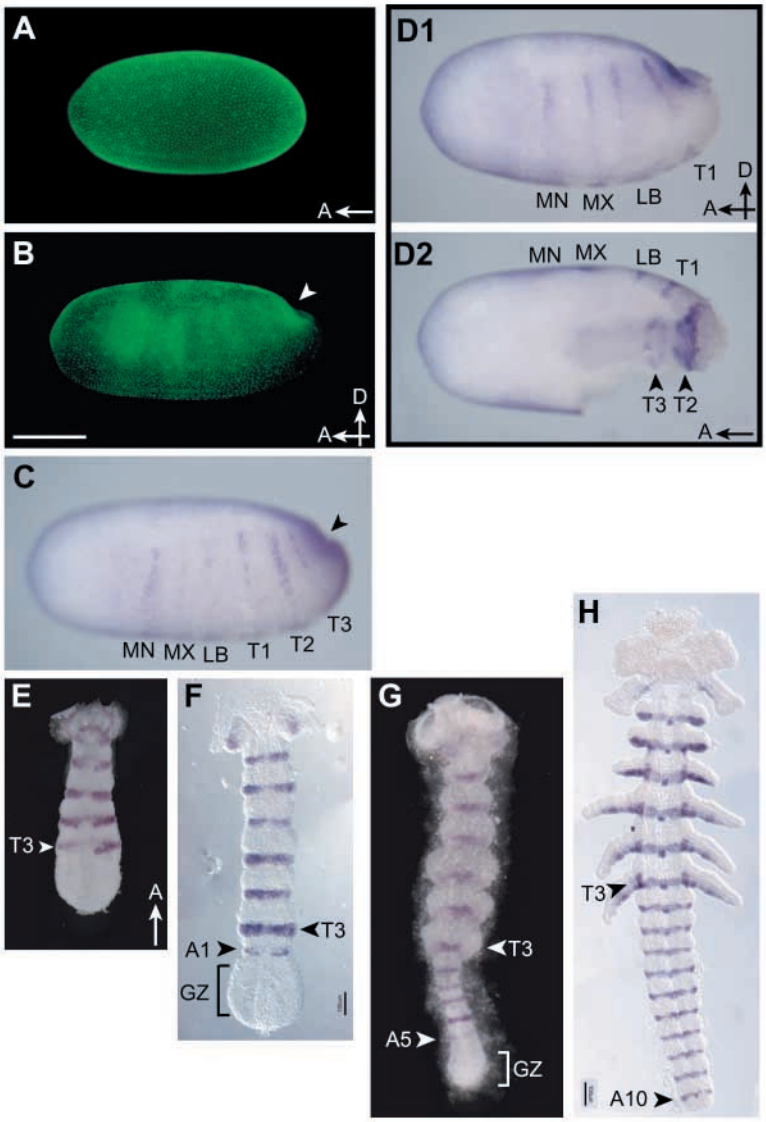

Fig. 1. *Oncopeltus* embryogenesis and *engrailed* expression. (A,B) Blastoderms stained with SYTOX to show nuclei. Anteroposterior axis and dorsoventral axis are indicated. (A) Early blastoderm at 24-28 hours. (B) Late blastoderm at 36-40 hours. Arrowhead indicates site of germband invagination. Scale bar: 200 μm. (C) Late blastoderm at 36-40 hours hybridized with *engrailed* probe (purple color). The six *en* stripes are labeled: MN, mandible; MX, maxillary; LB, labium; T1, first thoracic; T2, second thoracic; T3, third thoracic. Arrowhead indicates site of germband invagination. (D1) Embryo stained for *engrailed* at slightly later stage than in C. Note that only the four anterior *en* stripes are now visible on the blastoderm surface. (D2) Same embryo as in D1, with 'dorsal' region of blastoderm dissected away to reveal developing germband and rotated to view dorsal aspect. Note that the *en* stripes corresponding to the second and third thoracic segments are now on the invaginated germband. (E-H) Dissected germbands stained for *engrailed*, showing growth of the posterior and the sequential addition of the abdominal segments. Anterior is towards the top. (E) Early germband just completing germband invagination. (F) Forty-four- to 48-hour-old germband. A1, first abdominal *engrailed* stripe; GZ, posterior growth zone. (G) Embryo with five abdominal segments. (H) Fully elongated germband with the tenth and final abdominal *engrailed* stripe. Scale bar: 100 μm in F,H.

an anterior to posterior direction (Fig. 1E-H). This is similar to other short germband insects such as *Thermobia domestica*, *Schistocerca americana* and *Tribolium castaneum* (Brown et al., 1994; Patel et al., 1989; Peterson et al., 1998). Thus, it is clear that in *Oncopeltus*, as in other short and intermediate germband insects, posterior segments arise during a secondary growth phase during which the posterior germband undergoes great elongation with specification of abdominal segments occurring sequentially and in an anterior to posterior direction.

Milkweed bug *hunchback* gene structure

In order to clone *Oncopeltus hunchback* (*Of'hb*), we designed degenerate primers to the conserved zinc-finger domain of known *hunchback* sequences. We then performed PCR using these primers on cDNA made from ovaries or mixed stage embryos and isolated a short initial *Of'hb* clone. This clone allowed us to then design exact primers for 5′ and 3′ RACE and isolate fragments of *Of'hb* that together total 2.1kb and encode the entire open reading frame and regions of the 5′ and 3′ UTRs.

Of'hb is predicted to encode a 64.3 kDa protein with a total of eight zinc-finger domains. These zinc fingers are clustered with an N-terminal pair, a central cluster of four and a C-terminal pair (Fig. 2C). These eight zinc-finger domains are shared with the *hunchback* genes from two grasshopper species, *Locusta migratoria* and *Schistocerca americana*, while *Drosophila melanogaster* and *Tribolium castaneum hunchback* each encode only a total of six zinc fingers (Fig. 2A) (Patel et al., 2001; Tautz et al., 1987). The six fingers from the fly and beetle *hunchback* correspond to the central four and the C-terminal two fingers from the milkweed bug and the grasshoppers. Alignments of the homologous finger regions of grasshopper and milkweed bug *hunchback* show that the N-terminal zinc fingers are the most divergent.

As both the *Schistocerca* (Patel et al., 2001) and *Oncopeltus hunchback* encoded proteins contain eight zinc fingers, this is likely the ancestral state. However, *Tribolium* and *Drosophila hb* each contain only six zinc fingers, which suggests that six fingers is the ancestral state for the holometabola (Patel et al., 2001; Tautz et al., 1987; Wolff et al., 1995). If this is the case, then somewhere in the lineage leading to holometabola, *hunchback* lost its two N-terminal-most fingers (Fig. 2D). Unfortunately, as the function of the *hb* encoded protein itself has been studied only in *Drosophila* (which lacks these fingers), the function of these metal-binding fingers is unknown. It would be fascinating to examine the specific function of these ancient N-terminal fingers and see whether they can be correlated with developmental changes that have evolved in the holometabola.

In addition to the zinc-finger domains, three other domains were found to be conserved. The A-Box, originally identified in *Drosophila* as a region of similarity between *hunchback*, *Kruppel* and the HIV pol gene (Tautz et al., 1987), is also found

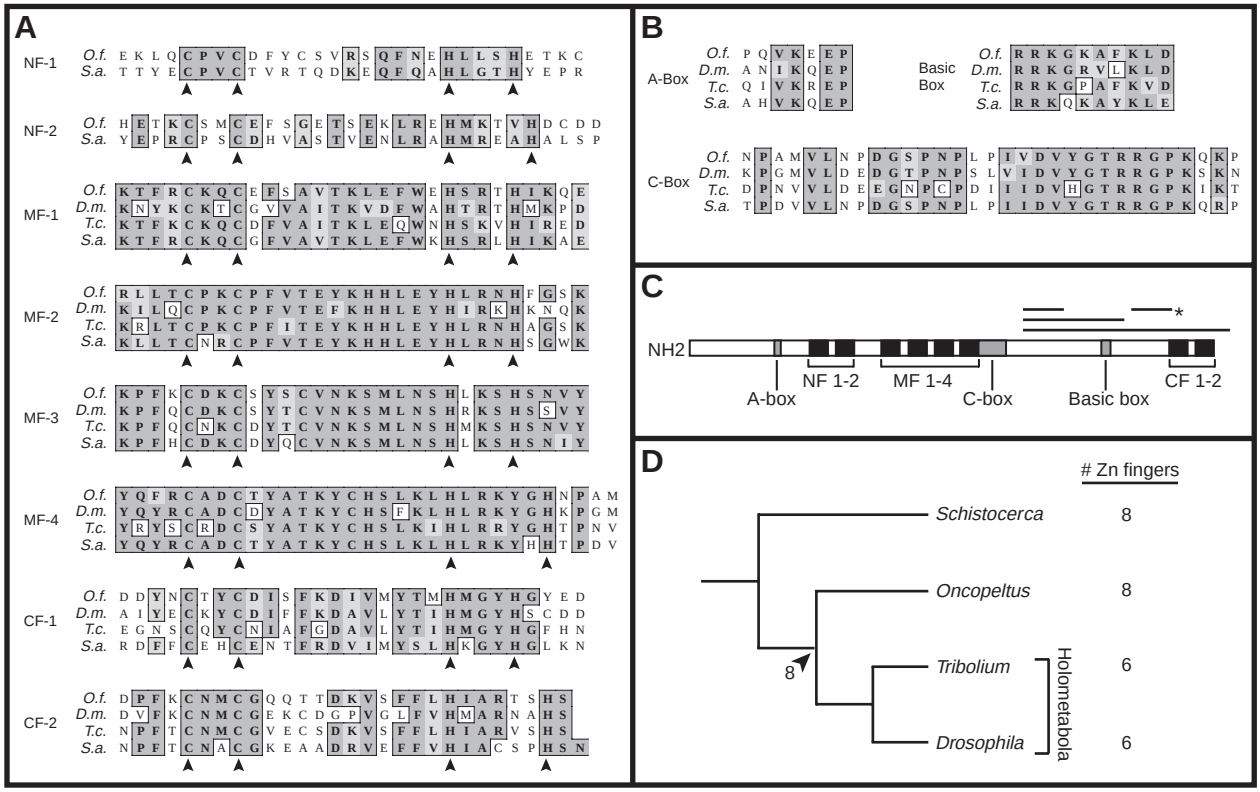

Fig. 2. Analysis of the *Oncopeltus fasicatus hunchback* sequence. (A) Predicted *Oncopeltus fasciatus hunchback* (*O.f.*) zinc-finger domains aligned with homologous domains from *Schistocerca americana* (*S.a.*), *Drosophila melanogaster* (*D.m.*), and *Tribolium castaneum* (*T.c.*). NF-1 and NF-2 are the amino-terminal two zinc fingers, MF 1-4 are the middle four fingers, and CF-1 and CF-2 are the carboxy fingers. Arrowheads indicate the locations of the critical cysteine and histidine residues. (B) Alignments of the *Oncopeltus* A-, Basic, and C-boxes with other insect species. (C) The predicted *Oncopeltus huncback* structure showing the locations of the zinc fingers (black boxes) and other conserved motifs (gray boxes). The locations of the 300 bp, 500 bp, and 1.1 kb dsRNA fragments used in RNAi are mapped above the protein structure. An asterisk indicates the second 300 bp fragment. (D) The predicted structures of insect *hunchback* proteins mapped upon the insect phylogeny. As both *Schistocerca* and *Oncopeltus hunchback* proteins are predicted to contain a total of eight zinc fingers, this is probably the ancestral state for the eumetabola (arrowhead). As *Tribolium* and *Drosophila hunchback* have only six zinc fingers, *hunchback* appears to have lost its two N-terminal fingers in the lineage leading to holometabola.

in *Oncopeltus hunchback*. Additionally, sequences similar to the *Drosophila hunchback* Basic Box and the C-Box are also present (Fig. 2B) (Hülskamp et al., 1994).

Of'hb transcript is maternally expressed and loaded into oocytes

Northern analysis on both maternally and zygotically derived total RNA revealed a single band of ~3.2 kb in both samples, showing that *Oncopeltus hunchback* is expressed in the ovary (Fig. 3A). As our Northern analysis shows the presence of a larger transcript than our cloned fragments (the 5′ and 3′ RACE products together total 2.1 kb), our clones must not represent the entire *Of'hb* transcript.

In situs on ovaries confirm our northern analysis and show that the *Of'hb* transcript is expressed in the ovary and developing oocytes. *Oncopeltus* ovaries are of the telotrophic type, meaning the nurse cells remain in the germarium, while the developing oocytes continue their journey of maturation down each ovariole. The nurse cells supply the oocytes with maternal factors through their connection via nutritive cords. Reflecting this morphology, ovarian in situs show that *hb* accumulates throughout the germarium and stain especially strongly within zone III (arrowhead in Fig. 3B), where the nurse cells are located (Bonhag and Wick, 1953). Transcript continues to accumulate and appears to be evenly distributed within the developing oocytes as they mature. *hb* becomes undetectable in late oocytes (Fig. 3B), but this absence of staining is probably due to chorion deposition around the mature oocytes as the chorion would present a physical barrier to probe and stain penetration.

Oncopeltus hunchback is expressed in two broad bands in the blastoderm

Oncopeltus hunchback expression occurs in a distinct blastoderm pattern and a separate germband pattern that reflects the distinct blastoderm and germband phases of milkweed bug embryogenesis. In early embryos before blastoderm formation (12 hours after oviposition at 25°C), *hb* transcript accumulates homogeneously throughout the egg (not shown). Shortly after, *hb* expression appears more strongly in the central region of the blastoderm (Fig. 4A). At 20-24 hours, this central domain becomes more strongly refined (Fig. 4B). By 24-28 hours, the single broad domain of expression begins to contract from the poles and resolve into two bands. The weaker, more anterior band spans 69-84% egg-length (with 0% being the posterior) while the stronger more central band

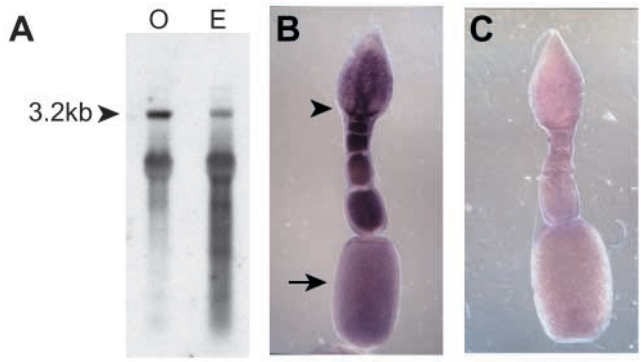

Fig. 3. *hunchback* is maternally expressed and loaded into developing oocytes. (A) Northern blot using a *hunchback* probe to ovarian (O) or embryonic (E) total RNA. A single band of 3.2 kb is detected. (B) In situ with *hunchback* probe on a single fixed ovariole. Arrowhead indicates zone III of tropharium, the area where the nurse cells are concentrated. Older oocyte (arrow) beginning to lay down chorion does not stain as strongly. (C) Ovariole in situ using sense control *hunchback* probe.

covers 40-64% egg-length (Fig. 4C). As *Oncopeltus* is an intermediate germ insect, this region of the blastoderm corresponds to different segments than what would be expected in a long germ insect, such as *Drosophila*. Thus, in order to determine the approximate segmental register of *Of'hb* expression on the blastoderm, images of milkweed bug embryos separately stained for *hunchback* and *engrailed* were juxtaposed. This allowed us to determine that the anterior band spans the region of the blastoderm anterior to the mandibular *en* stripe, while the posterior band of *hunchback* appears to span the maxillary and labial segments (Fig. 4E).

Also at this stage, although no overt morphological indentation can yet be seen, a posterior patch of *hunchback* transcript arises prefiguring the location of future germband invagination (arrow in Fig. 4C1). In late blastoderms and in embryos initiating germband invagination (32-40 hours), the two anterior stripes of *hb* begin to fade and the blastoderm shows *hb* staining in a speckled pattern (Fig. 4D). When the layer of cells that express the broad striped *hb* pattern are peeled from the yolk ball, it is clear that this speckled staining lies underneath the blastoderm layer (not shown). Therefore, this speckled pattern is due to accumulation in the underlying yolk cells. As the germband begins its invagination, this site also shows stain accumulation, which may be a continuation of the earlier posterior patch, or may simply be due to physical capture of stain by the folded tissues of the invagination.

Oncopeltus hunchback germband expression

During the germband phase of embryogenesis, *Oncopeltus hunchback* is expressed in a very different pattern than during blastoderm phase. If the broad blastoderm domains persisted through germband invagination, one would expect that in germbands, *hunchback* would likewise stain in a gap-like pattern in the gnathal/prothoracic region. Interestingly, this is not the case. From very early through very late germband stage embryos, *Of'hb* is never detected in an anterior gap gene-like domain (Fig. 5). Early germbands still undergoing invagination show very weak *hb* staining in a symmetrical chevron pattern which is segmentally reiterated and is excluded from the tip of the germband (Fig. 5A,B). This blocky segmental expression is most likely not a continuation of the earlier blastoderm domain but rather represents de novo expression in this new pattern. This expression is similar to a segmentally reiterated pattern also seen in *Musca* and *Tribolium* and may represent mesodermal staining as it does in *Schistocerca* (Patel et al., 2001; Sommer and Tautz, 1991; Wolff et al., 1995). As the broad bands of *Of'hb* expression in the blastoderm are already beginning to weaken by late blastoderm, it is likely that expression in these segments has already faded below detection by the time the germband completes invagination. This is in contrast to the *hunchback* expression patterns in both *Schistocerca* and in *Tribolium*, where it is expressed in a broad gap-like domain encompassing the gnathal to anterior first

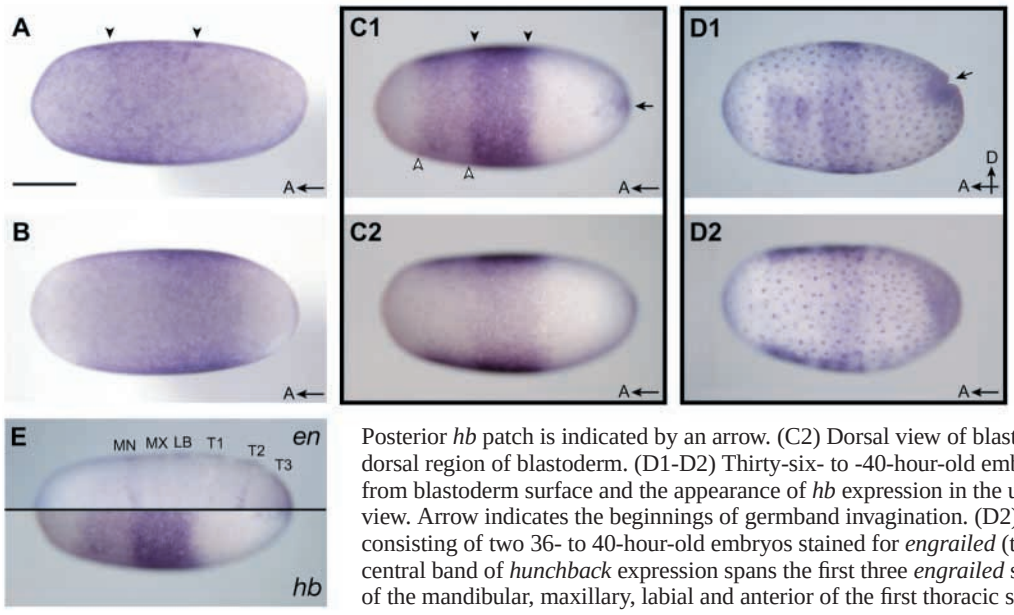

Fig. 4. *hunchback* blastoderm in situs. Anterior is towards the left in all images. (A) Twelve- to 16-hour-old blastoderm. *hb* transcript is diffuse along length of egg but is concentrated in the central region of the embryo (arrowheads). (B) Twenty- to 24-hour-old blastoderm. Accumulation in the central region of blastoderm becomes more pronounced. (C1-C2) Twenty-eight- to 32-hour-old embryo. (C1) Ventral view. Two bands of *hb* accumulation are apparent. Anterior and central bands (white and black arrowheads, respectively, are indicated. Posterior *hb* patch is indicated by an arrow. (C2) Dorsal view of blastoderm. *hb* expression is weaker in dorsal region of blastoderm. (D1-D2) Thirty-six- to -40-hour-old embryo. Bands of expression are fading from blastoderm surface and the appearance of *hb* expression in the underlying yolk nuclei. (D1) Lateral view. Arrow indicates the beginnings of germband invagination. (D2) Dorsal view. (E) Composite image consisting of two 36- to 40-hour-old embryos stained for *engrailed* (top) and *hunchback* (bottom). The central band of *hunchback* expression spans the first three *engrailed* stripes that correspond to the posterior of the mandibular, maxillary, labial and anterior of the first thoracic segments. Scale bar: 200 μm.

thoracic segments in early germbands (Patel et al., 2001; Wolff et al., 1995).

During germband elongation, *Oncopeltus hunchback* is expressed strongly in a patch at the very posterior of the germband. This posterior domain of *hb* expression begins as two small dots at the tip of the elongating germband (Fig. 5C). Double staining with *engrailed* shows that these dots only appear after the first abdominal segment has already formed. These two spots quickly expand to form a half-moon shape (Fig. 5D) that persists continuously throughout germband extension and can be detected until the formation of the tenth and final abdominal *engrailed* stripe (Fig. 5F). This continuous expression suggests that *hunchback* may be required in the growth zone throughout germband elongation.

Earlier, just before germband invagination, there is a small patch of *hunchback* expression in the posterior of the blastoderm (arrow in Fig. 4C1). As *hb* is expressed in the posterior growth zone during abdomen formation, these two domains may at first glance seem to represent continuous *hb* expression. However, this is not the case as early germbands, which are just beginning the invagination process, do not express *hb* at the posterior tip (Fig. 5A,B). It is only after invagination is complete and during the formation of the abdominal segments that *hb* expression reappears in the growth zone. Therefore, these two domains cannot represent a *continuous* expression of *hb*. Rather, the patch of expression in the 'growth zone' must represent a de novo initiation of *hunchback* transcription.

hunchback is also expressed in a pattern that may represent the developing nervous system. The punctate pattern in late germbands are reminiscent of neural expression patterns and are consistent with *hb* neural expression in other insects and its function in *Drosophila* (Isshiki et al., 2001; Patel et al., 2001; Wolff et al., 1995). This neural-like expression suggests that *hunchback* is also required for neurogenesis in *Oncopeltus*.

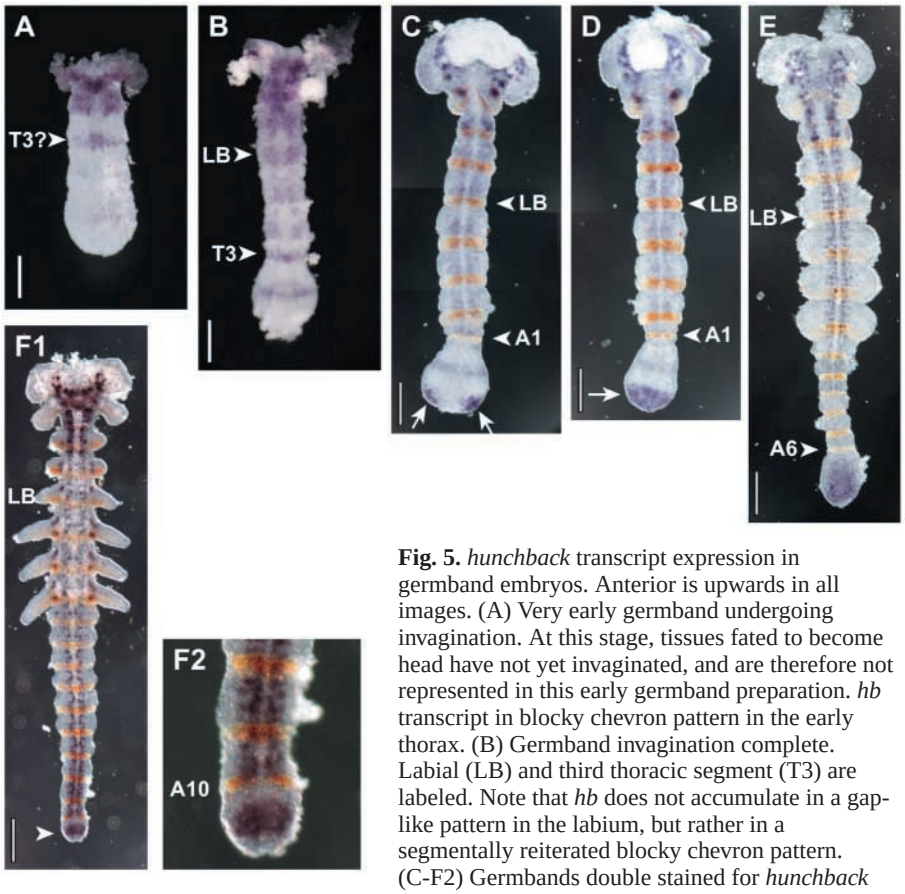

Fig. 5. *hunchback* transcript expression in germband embryos. Anterior is upwards in all images. (A) Very early germband undergoing invagination. At this stage, tissues fated to become head have not yet invaginated, and are therefore not represented in this early germband preparation. *hb* transcript in blocky chevron pattern in the early thorax. (B) Germband invagination complete. Labial (LB) and third thoracic segment (T3) are labeled. Note that *hb* does not accumulate in a gap-like pattern in the labium, but rather in a segmentally reiterated blocky chevron pattern. (C-F2) Germbands double stained for *hunchback* (purple) and *engrailed* (orange). (C) Germband beginning elongation. Labial (LB) and first abdominal (A1) segments are labeled. Arrows indicate two dots of *hb* expression in the posterior zone. (D) Slightly later embryo than in C, posterior dots of *hb* have now expanded to become a half-moon patch in the posterior (arrow). (E) *hunchback* expression persists throughout germband extension. The sixth abdominal segment (A6) is labeled. Also note that *hunchback* is now expressed in a neural pattern in the trunk of the germband. (F1) *hunchback* is expressed in the posterior until the formation of the tenth abdominal segment (arrowhead). (F2) Close up of posterior germband in (F1). Scale bars: 200 μm in A-F1.

Oncopeltus parental RNAi

Recently, it has been reported that female *Tribolium* pupa which had been injected with double-stranded RNA (dsRNA) produce progeny showing an RNAi knockdown phenotype (Bucher et al., 2002). In order to test this method in *Oncopeltus*, we injected dsRNA corresponding to a region of *Oncopeltus Sex combs reduced* (*Of'Scr*), a homeotic gene, into the abdomens of adult virgin females and scored their progeny for defects. These progeny had their labial appendages transformed into a pair of appendages of mixed leg/antennal-like identity (Fig. 6B) – a phenotype identical to that already published for *Of'Scr* by direct injection of dsRNA into early embryos (Hughes and Kaufman, 2000). We achieved much higher penetrance and a similar range of phenotypes using parental RNAi (pRNAi) when compared with embryonic RNAi (eRNAi). All surviving injected females eventually produced clutches of embryos with the *Scr* phenotype and these animals showed the complete range of defects as reported earlier using embryonic RNAi. Sometimes, the first clutch laid contained wild-type hatchlings – most likely because these eggs had already completed oogenesis and laid down their chorions that would be impenetrable to dsRNA. These same females would later go on to lay clutches that did show the *Scr* knockdown phenotype. We also found that over the span of about 3 weeks, the severity of defect would first increase, peaking around at 10 days post-injection and then gradually decrease after that (Fig. 6C). As pRNAi showed identical phenotypes as eRNAi without any injection artifacts and showed the full range of severity, this technique should prove to be a highly specific and convenient method for studying gene function in *Oncopeltus*.

hunchback RNAi

In order to determine the functional role of *hunchback* during *Oncopeltus* embryogenesis, we used RNAi to deplete the *hb* transcript and produce knockdown phenotypes. As parental RNAi does not

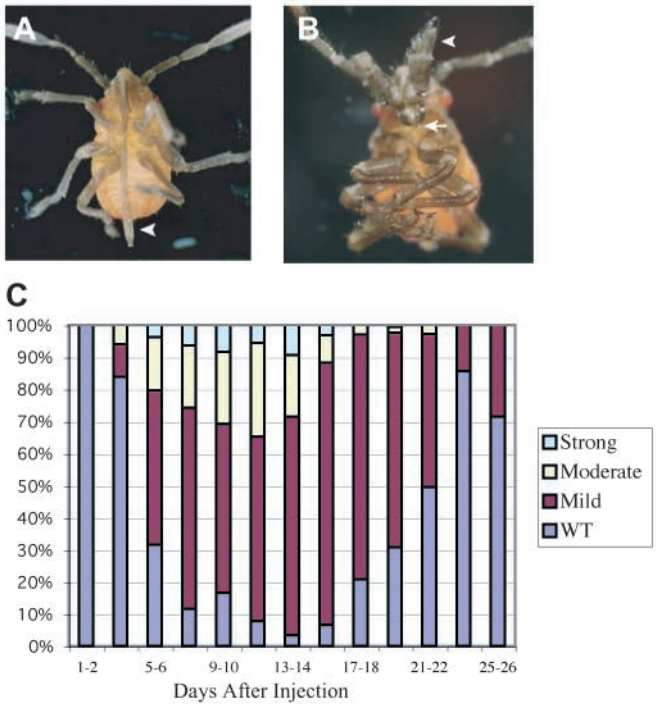

Fig. 6. Testing parental RNAi with *Oncopeltus Sex combs reduced* (*Of'Scr*). (A) Hatchling from uninjected mother. Arrow indicates labium. (B) *Of'Scr* pRNAi hatchling. Arrowhead indicates transformed labium. Arrow indicates normal stylet. For a full description of the *Of'Scr* phenotype, see Hughes and Kaufman (Hughes and Kaufman, 2000). (C) Time course for *Of'Scr* pRNAi. X-axis is number of days the clutch was laid after injection of the female. *y*-axis is percent that each phenotypic category contributed to the total. The RNAi effect peaks around ten days after injection and declines after that.

yield any injection artifacts, we preferred to use pRNAi but had to first confirm that for *hunchback*, pRNAi and eRNAi produced equivalent phenotypes. We found that for *Of'hb*, as for *Of'Scr*, no qualitative difference in the phenotypes were produced by either technique (Table 1). In order to test the effect of dsRNA length, we also injected several overlapping *hb* dsRNAs of varying length – 300 bp, 500 bp and 1.1 kb (Fig. 2C), and found that the resulting phenotypes from all the fragments were again qualitatively identical. However, we did find that the shorter fragments gave slightly more severe phenotypes (Table 1 – compare the frequency of classes IV and V for the 300 bp fragment and the 1.1 kb fragment). Moreover, a different 300 bp dsRNA fragment was tested individually and also pooled with the first 300 bp fragment and each gave the same qualitative phenotype as the other longer fragments. As both pRNAi and eRNAi gave identical phenotypes and all the differently sized dsRNA fragments tested also yielded the same defects, we are confident that they truly represent depletion of the *hunchback* gene product.

RNAi with *Oncopeltus hunchback* resulted in phenotypes that ranged in severity from wild-type to very severe, and we were able to categorize the resulting embryos into five phenotypic classes based on this range of phenotypic severity. This allowed us to arrange a hypomorphic series of *hunchback* function that aided our interpretation of the phenotype. The

Table 1. Results of parental and embryonic *hunchback* RNAi

	dsRNA size	Undeveloped or nonspecific		Wild type		Class I		Class II		Class III		Class IV		Class V		Total
hb pRNAi	300 bp	1 (1.4)		0 (0)		3 (4.2)		29 (40.3)		12 (16.7)		20 (27.8)		7 (9.7)		72
	300+300 bp	2 (2.9)		0 (0)		0 (0)		23 (33.3)		11 (15.9)		10 (14.5)		23 (33.3)		69
	500 bp	13 (7.3)	18 (4.0)	0 (0)	0 (0)	19 (10.7)	38 (8.4)	88 (49.7)	196 (43.1)	31 (16.4)	90 (19.8)	21 (11.9)	67 (14.7)	5 (2.8)	46 (10.1)	175
	1.1 kb	2 (1.5)		0 (0)		16 (11.7)		56 (40.9)		36 (26.3)		16 (11.7)		11 (8.0)		137
hb eRNAi	300+300 bp	27 (43.5)		0 (0)		7 (11.3)		6 (9.7)		3 (4.8)		2 (3.2)		17 (27.4)		62
	500 bp	47 (52.2)	227 (55.6)	1 (1.1)	8 (2.0)	13 (14.4)	49 (12.0)	10 (11.1)	43 (10.5)	5 (5.6)	17 (4.2)	2 (2.2)	13 (3.2)	12 (13.3)	51 (12.5)	90
	1.1 kb	153 (59.8)		7 (2.7)		29 (11.3)		27 (10.5)		9 (3.5)		9 (3.5)		22 (8.6)		256
Totals for pRNAi+eRNAi		245 (28.4)		8 (0.9)		87 (10.1)		239 (27.7)		107 (12.4)		80 (9.3)		97 (11.2)		863

Results show number of embryos of given phenotypic class with percentages in parentheses.
Percentages may not add up to 100% because of rounding.
300+300 bp refers to injection with a pool of dsRNA solution containing the two different 300 bp fragments.
Phenotypic classification was determined based on severity of phenotype, with class V being the most severe.
The 'Undeveloped or nonspecific' classification included embryos that failed to develop or showed uninterpretable defects. The high frequency of this class in the eRNAi experiment is probably the result of lethality caused by injection, as a similar rate was found with embryonic injections with other genes and with buffer (data not shown) (see Hughes, 2000).

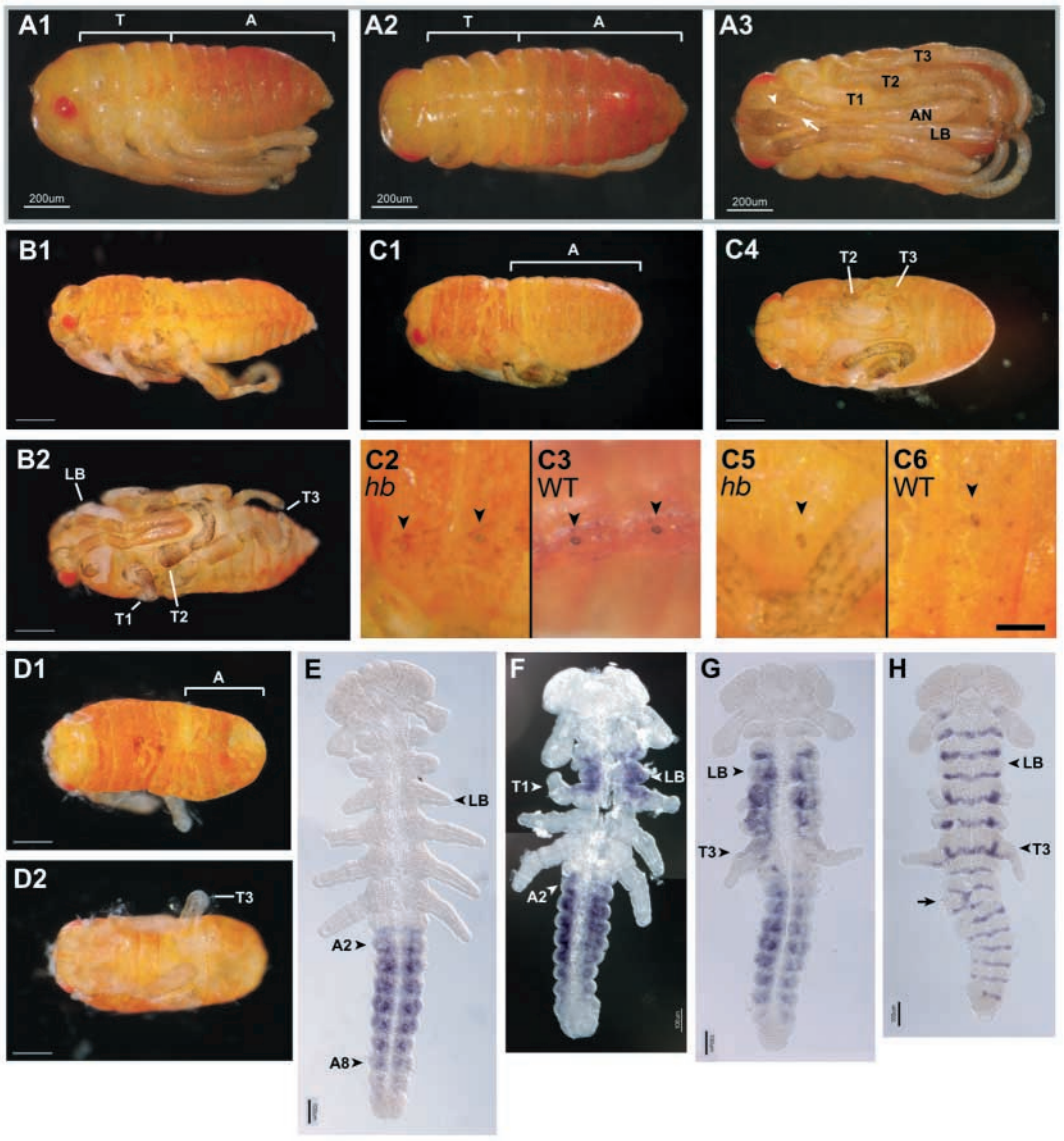

Fig. 7. Class I-III (mild and moderate) *hunchback* RNAi phenotypes. (A1-A3) Uninjected embryos. Anterior towards the left. Thoracic and abdominal regions are delineated. (A1) Lateral view. (A2) Dorsal view. (A3) Ventral view. Arrowhead indicates the mandibular stylet, arrow indicates the maxillary stylet. AN, antenna; LB, labium; T1, first thoracic leg; T2, second thoracic leg; T3, third thoracic leg. (B1-B2) Class I embryo. (B1) Lateral view. (B2) Ventral view. Labium is a lump of undifferentiated tissue. T1 leg is reduced, while T2 and T3 legs are less strongly affected. (C1,C2,C4,C5) Class II embryo. (C1) Lateral view. Abdominal region indicated. (C2) Close-up of gnathal and anterior thorax of embryo in C1. Arrowheads indicate abdominal-like spiracles. (C3) Close-up of abdominal spiracles (arrowheads) on uninjected animal. (C4) Ventral view of embryo shown in C1, C2. Reduced second and third thoracic legs are labeled. (C5) Close-up of gnathal region of embryo shown in C4. Arrowhead indicates location of ventral fourth abdominal (A4) spiracle. (C6) Close up of A4 of uninjected animal. Spiracle indicated with arrowhead. Scale bar: 50 μm. (D1-D2) Class III embryo. (D1) Dorsal view. Note dorsal segmentation defect. Abdominal region indicated. (D2) Ventral view. Defective third thoracic leg (T3) is labeled. Note abdominal-like segmentation in gnathal region of animal. (E) Wild-type germband stained for *abdominal-A*. Note expression in second through eighth abdominal segments and lack of expression in labial segment. (F) Putative class I embryo stained for *abd-A*. Note reduced labium (LB). (G) Putative class III embryo stained for *abd-A*. (H) Putative class II embryo stained for *engrailed*. Scale bars: 200 μm in A-C1,C4,D; 50 μm in C6; 100 μm in E-H.

Of'hb RNAi phenotype consisted of two aspects, which we will describe in turn.

hunchback suppresses abdominal identity

The first aspect of the *hunchback* depletion phenotype is a homeosis of the gnathal and thoracic regions towards abdominal identity. Class I embryos (the weakest phenotypic class) made up 8.3% of the embryos (Table 1). These embryos showed strong suppression of the labium and mildly defective first thoracic legs (Fig. 7B1,B2). The fact that the labial segment is most strongly affected demonstrates that this segment is at the epicenter of defect and is consistent with the strong band of *hunchback* expression spanning the maxillary through anterior prothoracic segments in the blastoderm.

Embryos with a moderate RNAi defect constituted classes II and III and together totaled 43.3% of all the embryos (Table 1). In these embryos, in addition to the labial defects, it appears that the region of defect has expanded to include the anterior thoracic regions. Appendages on these segments are suppressed and deformed while the body segments begin to adopt abdominal features. For example, in class II embryos, the pigmentation of the gnathal region and anterior thorax begins to resemble that of the abdomen (compare Fig. 7C1 with Fig. 7A1) and spiracles of abdominal identity and position are apparent in the gnathal region (Fig. 7C2,C3). Furthermore, a ventral spiracle that in wild-type animals is present on the fourth abdominal sternite is ectopically produced in the transformed thoracic region of affected animals (Fig. 7C5,C6). In the more severe class III embryos, the region of defect expands to encompass more of the thoracic region, resulting in increased suppression of the first and second legs often leaving only the third leg (Fig. 7D2). In addition, ventral segmentation appears abdominal like (Fig. 7D2) showing that abdominal transformation of these segments is nearly complete. Additionally in these animals, dorsal segmental defects are occasionally seen (Fig. 7D1). Thus, at the morphological level, these *hunchback* hypomorphs show a transformation of the labial and thoracic segments towards abdominal identity.

We reasoned that transformation of the gnathal and thoracic regions towards abdomen should be accompanied by expression of abdominal genes in these transformed segments. In wild-type animals, the homeotic gene *abdominal-A* (*abd-A*) is expressed in the abdomen from the second through eighth abdominal segments (Fig. 7E). Therefore, we examined the expression domains of *abd-A* in embryos that were depleted for *hunchback*. Although we did not detect *abd-A* expression during the blastoderm stage in *hb* RNAi embryos (data not shown), we did find ectopic expression of *abd-A* during the germband stage. In *hb*-depleted germband stage embryos, *abd-A* was ectopically expressed in the gnathal and anterior thoracic segments, coincident with suppression of appendages on these segments (Fig. 7F,G). In weaker hypomorphs, the ectopic domain spanned the posterior of the maxillary segment through the anterior of the first thoracic segment and leg (Fig. 7F). In more strongly affected RNAi embryos, the ectopic domain of *abd-A* was more expanded – into the first and second thoracic segments and was associated with suppression of legs on these segments (Fig. 7G).

The ectopic expression of *abd-A* shows that *hb* RNAi embryos at both the morphological and molecular level show a homeosis of the labium and thorax towards abdominal identity. Moreover the hypomorphic series shows that the domain of transformation starts at the labial and first thoracic segments in weakly affected animals, expands posteriorly to include the second thoracic segment in moderately affected ones, and incorporates the third thoracic segment in strong hypomorphs, which suggests that the labial and first thoracic segments are the most sensitive to *hunchback* depletion.

Severe *hunchback* depletion results in posterior compaction

In addition to the anterior homeotic transformations described above, *hunchback* depletion revealed another defect apparent in the abdomen. Decreasing *hb* activity results in increased posterior compaction. This defect is most evident through the hypomorphic series where a trend towards smaller and more defective abdominal segments in stronger phenotypic classes is apparent. Whereas class I embryos show a largely wild-type abdomen (Fig. 7B1), class II embryos show mild compaction of the abdomen (compare Fig. 7C1 with 7A1). This compaction increases and is often associated with segmental defects in class III embryos (Fig. 7D1). Embryos of stronger phenotypic classes are smaller than normal overall, and the abdomen shows much stronger compaction (compare the *hb* RNAi embryos in Fig. 8A,C2,D to the uninjected animals in Fig. 7A1,A2). In class IV embryos, a tiny and deformed posterior leg is often situated near the extreme posterior of the animal (Fig. 8B,C1). As the third thoracic segment is the last to be transformed and its leg is most resistant to suppression, this posterior appendage is most likely the partially suppressed remnants of the third thoracic leg. In these animals, the gnathal and anterior thoracic segments are strongly transformed towards abdomen, resulting in suppression of their appendages, while the third thoracic segment is only partially transformed, leaving a remnant of the third leg. Therefore, the posterior position of these stubby legs underscores the extreme degree of posterior compaction in these animals. Coupled with the homeosis described above, strongly affected animals would thus have a normal head followed by several abdominal-like segments that consist of a transformed labium and thorax and a tiny compacted abdomen.

This posterior compaction is perhaps most clearly seen during embryogenesis, with staining for *engrailed*. By using the degree of gnathal and thoracic appendage suppression as an indicator for phenotypic severity, we can see (as judged by disruptions in *Of'en* expression) that abdominal segmentation becomes more defective in more severely affected animals. Putative class II animals show mild defects in abdominal segmentation (Fig. 7H), while class IV (Fig. 8F) and class IV/V (Fig. 8G) animals show more strongly affected abdominal patterning. These defects may be the cause of the posterior compaction seen at the morphological level. Although the abdomens of *hunchback*-depleted embryos can be severely compacted, it does not seem that this compaction is merely due to a precocious termination of segmentation. If precocious termination were the case, we would expect fewer but relatively normal abdominal segments. Therefore, it is possible that *hunchback* is somehow required for normal posterior growth with the segmentation defect occurring as a consequence of this. Importantly, while segmentation in the abdomen is defective, it is apparent that segmentation is normal in the gnathal and thoracic segments (see Fig. 7H, Fig. 8F,G). Although the appendages of these segments are suppressed, their morphology and *engrailed* expression appear otherwise normal.

The most severe class of animals comprised 11.3% of the total (Table 1) and the interpretation of this class is based somewhat on an extrapolation of the hypomorphic series. These embryos are extremely small and are found buried in the yolk mass. In normal embryogenesis, the germband undergoes dorsal closure to encircle the yolk so in the wild-type case, the yolk mass ends up inside the embryo. In class V embryos, it appears instead that the embryo develops without enveloping the bulk of the yolk and thus much of the egg space is filled with unused yolk. Upon closer examination of these embryos it seems that some internal organs may have actually developed on the outside of the embryo, similar to the 'everted' embryos described by Sander (Sander, 1976). In this class of animals, only the anterior-most structures are clearly identifiable. Eyes

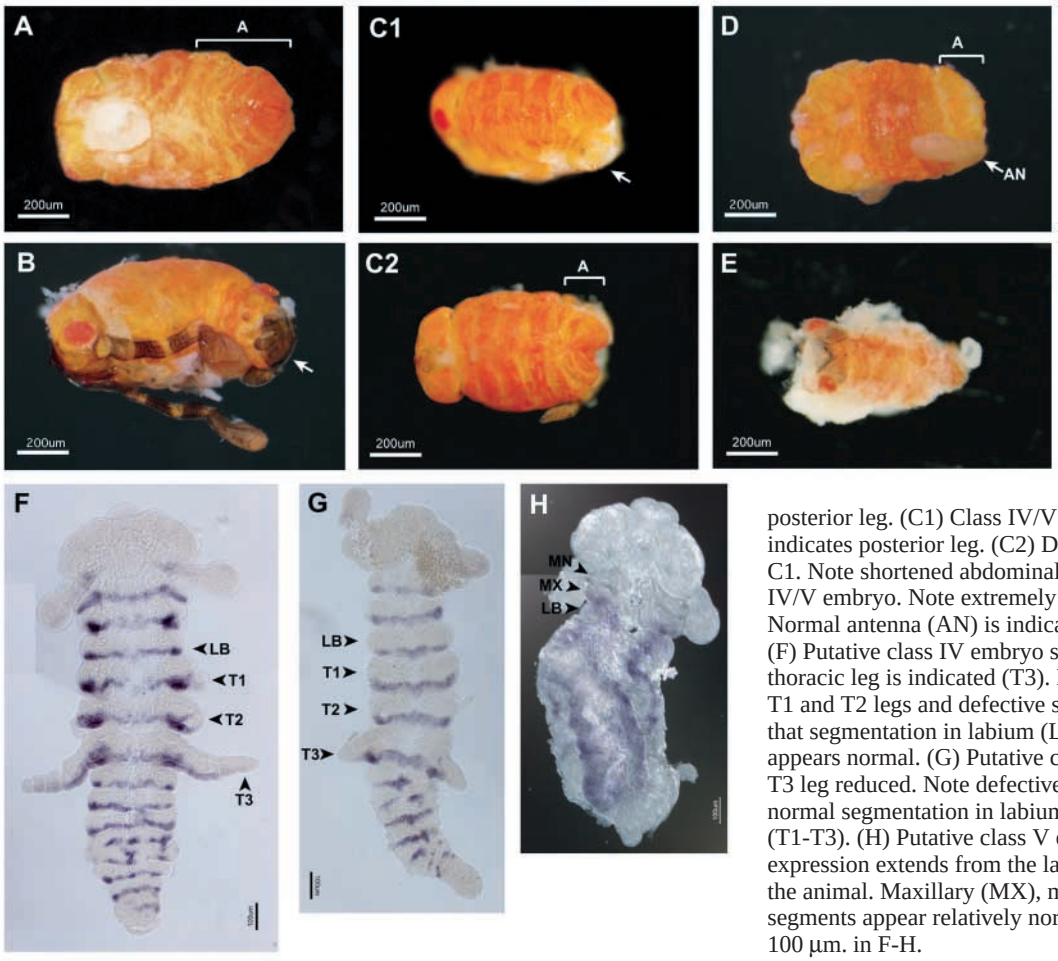

Fig. 8. Class IV and V embryos. (A) Dorsal view of class IV embryo. This embryo did not complete dorsal closure. Note defective segmentation and shortened abdominal region. (B) Class IV embryo. Arrow indicates posterior leg. (C1) Class IV/V embryo. Lateral view. Arrow indicates posterior leg. (C2) Dorsal view of embryo in panel C1. Note shortened abdominal region. (D) Dorsal view of class IV/V embryo. Note extremely shortened abdominal region. Normal antenna (AN) is indicated. (E) Class V embryo. (F) Putative class IV embryo stained for *engrailed*. Third thoracic leg is indicated (T3). Note highly reduced labium and T1 and T2 legs and defective segmentation in abdomen. Note that segmentation in labium (LB) and thoracic region (T1-T3) appears normal. (G) Putative class IV/V embryo stained for *en*. T3 leg reduced. Note defective segmentation in abdomen and normal segmentation in labium (LB) and thoracic region (T1-T3). (H) Putative class V embryo stained for *abd-A*. *abd-A* expression extends from the labial segment to the posterior of the animal. Maxillary (MX), mandibular (MN) and labial (LB) segments appear relatively normal. Scale bars: 200 μm in A,E; 100 μm. in F-H.

and antenna develop, but the rest of the body is highly reduced and composed of fewer and smaller segments (Fig. 8E). It is important to note that although this body region is small, it is apparent that some segmentation has occurred. In a putative class V germband, segmentation of the anterior is apparent, with a few anterior segmental grooves clearly forming (arrows in Fig. 8H). This region of somewhat normal segmentation is followed by a highly defective region. *abd-A* in situs show that aside from the head and mandibular segments, the entire trunk expresses *abd-A*. Therefore, in this extreme class of *hb* depletion, posterior segmentation is highly defective and all of the post-maxillary body has adopted an abdominal fate. This phenotypic class may represent the most severe combination of the two aspects of *hunchback* depletion where the labial and thoracic segments are completely transformed towards abdominal identity and the abdomen has been severely compacted. This results in an animal in which the head is followed by a small number of segments, all of which have abdominal identity.

Our complete model including both aspects of *hunchback* function in *Oncopeltus* is presented in Fig. 9. We propose that as *Of'hb* function is depleted, first the labium and then the thorax is transformed towards abdominal identity. A second requirement is evident in the abdomen. In increasingly severe *hb* depletions, growth and segmentation in the abdomen becomes increasingly defective resulting in posterior compaction. In addition, apparent is a lack of clear segmental defects in the gnathal and thoracic regions, even in strongly affected animals. Therefore, in the most severe cases, a normal head is followed by a few segments of abdominal identity. Although this would at first glance appear to mimic the *hunchback* gap phenotype in *Drosophila* and *Tribolium*, we conclude that the strongest phenotype is due to the combination of gnathal and thoracic transformation towards abdomen coupled with severe posterior compaction.

Discussion

At first glance, the *Oncopeltus* blastoderm seems to resemble that of *Drosophila*. It is easy to imagine that developmental mechanisms instructing embryogenesis would be conserved between these species. However, since milkweed bugs undergo intermediate germband segmentation, there are fundamental differences between patterning in these two species. *Oncopeltus* embryogenesis consists of two distinct phases – a blastoderm phase and a germband phase and is reflected in the expression of *engrailed*. Our *engrailed* staining reveals that in *Oncopeltus*, the blastoderm has only been allocated into six anterior segments and confirms the milkweed bug's status as an intermediate germband insect. Moreover, the fact that *engrailed* transcript can be detected at all during the blastoderm stage shows that the degree of anterior patterning has progressed all the way to level of the segment polarity genes. This means that molecular

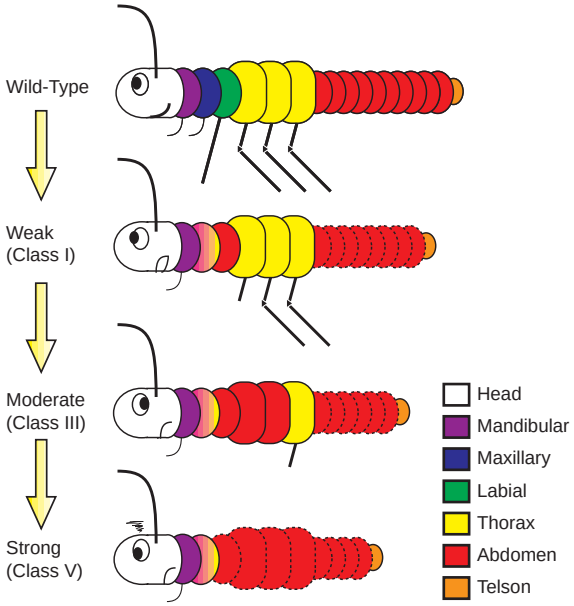

Fig. 9. Model for *hunchback* depletion in *Oncopeltus fasciatus*. Increasingly stronger *hunchback* knockdown results in two distinct effects. The first aspect of the depletion phenotype is transformation of the labial and anterior thoracic segments towards abdominal identity. In stronger depletion animals, this region of transformation expands, eventually encompassing the entire thorax. The second aspect of the *hunchback* phenotype is posterior compaction. Weak *hb* depletion results in mild compaction of the abdomen. In moderate and strong phenotypic classes, the abdomen is significantly shortened, with associated defects in segmentation. Therefore in the most severe cases (class V), these two aspects together result in a phenotype where the head is followed by an indeterminate number of segments, all with abdominal identity.

patterning of the anterior segments is essentially complete at a stage where the posterior body regions do not yet even exist. Thus, milkweed bugs show a severe heterochronic discontinuity between anterior and posterior segmental patterning. This anteroposterior discontinuity is in marked contrast to *Drosophila*, where by the completion of the blastoderm stage, the entire body region is proportionally represented and segmental patterning occurs more or less simultaneously across the entire blastoderm (Lohs-Schardin et al., 1979).

Oncopeltus hunchback expression and function in the labium and thorax

Oncopeltus hunchback expression and function reflect the biphasic nature of milkweed bug embryogenesis. *hb* is expressed in two broad stripes during the blastoderm stage. The stronger band spans the posterior maxillary, labial and anterior first thoracic segments. As *hb* is not expressed in these segments during the germband stage (except in the mesoderm and a neural-like domain), we attribute its region-specifying function in these segments to its expression domain in the blastoderm. This abdomen-repression function in the labial and thoracic segments may occur either through direct suppression of *abd-A* in the anterior, or may occur indirectly through regulation of a downstream gene responsible for specifying abdominal regional identity. As the ectopic domain of *abd-A* in *hb* RNAi animals was not detected at the blastoderm stage but only later during the germband stage and the region of homeosis in *hb* RNAi animals is much larger than the *hb* blastoderm expression domain, it is most likely that *hb* indirectly regulates *abd-A*. Indeed, normal *abd-A* expression in the abdomen appears long after *hb* expression in the growth zone has already faded. Our observation that *hunchback* in milkweed bugs serves to repress abdominal identity is not without precedence. In *Drosophila*, certain hypomorphic alleles of *hunchback*, class V alleles, also produce homeotic transformations of the gnathal or thoracic segments (Jürgens et al., 1984; Lehmann and Nüsslein-Volhard, 1987). However, unlike *Oncopeltus*, these transformations are superimposed on a deletion phenotype.

As in flies, *hunchback* RNAi depletion in the red flour beetle, *Tribolium castaneum*, also produces the gnathal and thoracic gap phenotype (Schröder, 2003). In this light, it is interesting that *Oncopeltus hunchback* knockdowns do not show the canonical gap phenotype but rather a transformation. This may reflect either incomplete RNAi knockdown of the *Of'hb* gene product or may reflect differences in anterior-posterior patterning in milkweed bugs. It is possible that if further depletion were possible, the anterior homeotic phenotype would be replaced by deletion of those segments. However, this would be in contrast to the case in *Drosophila* as weak alleles of *hunchback* in flies are not associated with transformations but rather yield small deletions while stronger alleles serve to increase the size of the deleted region (Lehmann and Nüsslein-Volhard, 1987). The *Oncopeltus hunchback* phenotype reported here seems to reflect a strong depletion of the *hunchback* gene product because of the large domain of the homeotic defect from the labium to the third thoracic segment in the severe phenotypic classes. Transformation of the third thoracic segment is indicative of strong *hb* RNAi yet in these same animals, the labial segment is present and without segmental defects. If deletion of the labial segment were merely an issue of sensitivity, we would expect that animals with transformed third thoracic segments also show segmental defects in the labial segment. Therefore, if *hunchback* has a gap function in this animal, its requirement must be minimal.

We have shown that *hunchback* transcript is provided maternally in *Oncopeltus* and it is a formal possibility that the protein is as well. If this were the case, it is possible that maternal *hunchback* serves to specify the presence of the gnathal and thoracic segments, while zygotic activity functions to suppress abdominal identity in these regions. Although maternal loading of *hunchback*-encoded protein has not been reported in either flies or beetles, the protein is provided maternally in grasshoppers. In grasshoppers however, axial patterning by *hunchback* appears to be performed entirely by zygotic function whereas maternal *hunchback* activity in this animal may serve to distinguish embryonic from extra-embryonic cells (Patel et al., 2001).

Oncopeltus hunchback expression and function in the growth zone

In strongly affected *Oncopeltus hunchback* RNAi animals, the abdomen is severely compacted and segmentation is defective. *hunchback* function in the developing germband probably reflects its expression in the posterior 'growth zone'. Therefore we propose that *Of'hb* is required for proper growth and segmentation of the posterior germband. At this time we can

only speculate on the nature of this requirement. It may be that *Of'hb* is directly involved in the generation of segments as the posterior germband grows. However, it may also be that *Of'hb* is merely required for posterior elongation of the germband while the actual patterning of segments occurs relatively independently of growth. Thus, the segmental defects seen in developing germbands may be a consequence of improper elongation. Alternatively, *hunchback* may be required for proper functioning of the growth zone itself.

hunchback has also been examined in *Schistocerca* and *Tribolium*, two other short germband insects. *Schistocerca hunchback* is not expressed continuously in the growth zone as it is in both milkweed bugs and beetles but rather arises in abdominal patches corresponding to the A4/A5 and A7-A9 segments (Patel et al., 2001). Therefore the continuous expression in the growth zone may represent a derived pattern in the insects. As noted, *Tribolium* and *Oncopeltus hunchback* are expressed in identical patterns in the growth zone. However, it has not yet been reported that *hb* RNAi in *Tribolium* leads to posterior compaction, rather the phenotype reported is the canonical *hunchback* gap phenotype. With such disparate expression and functional data from these three insects, it is difficult to determine the ancestral function of *hunchback* in the insect growth zone and it is clearly imperative that wider taxonomic sampling needs to be done.

This brings us to examinations of the very nature of the insect growth zone itself. Almost nothing is known about how this special region of the germband develops and ultimately gives rise to the posterior segments. There are no overt morphological features that distinguish it. However, the growth zone must be special as several segmentation genes such as *even-skipped*, *caudal* and *hunchback* are expressed there (Dearden and Akam, 2001; Patel et al., 1994; Wolff et al., 1995) (P.Z.L., unpublished). Given that some form of short germband development is ancestral in insects, we must understand this mode of development in order to understand the evolutionary transition from short to long germ segmentation. Moreover, as other arthropods undergo embryogenesis in a manner similar to insect short germband segmentation, functional studies in *Oncopeltus* and other short germband insects may in fact shed light on *all* the arthropods.

We thank Cynthia L. Hughes and David R. Angelini for critical reading of the manuscript. We also thank two anonymous reviewers whose comments and expertise were very helpful. Equipment and facilities used in this work were partially supplied by INGEN funding. P.Z.L. was supported by an NIH Genetics Training Grant GMO7757 and an NSF Integrative Graduate Education and Research Traineeship (IGERT) 2039L1A-A1. T.C.K. is an HHMI Investigator.

References

Bonhag, P. F. and Wick, J. R. (1953). The functional anatomy of the male and female reproductive systems of the milkweed bug, Oncopeltus fasciatus (Dallas) (Heteroptera: Lygaeidae). *J. Morphol.* **93**, 177-283.

Brown, S. J., Patel, N. H. and Denell, R. E. (1994). Embryonic expression of the single Tribolium engrailed homolog. *Dev. Genet.* **15**, 7-18.

Bucher, G., Scholten, J. and Klingler, M. (2002). Parental RNAi in Tribolium (Coleoptera). *Curr. Biol.* **12**, R85-R86.

Butt, F. H. (1947). Embryology of the Milkweed Bug *Oncopeltus fasciatus* (Hemiptera). *Cornell Experiment Station Memoir* **283**.

Davis, G. K. and Patel, N. H. (2002). SHORT, LONG, AND BEYOND: molecular and embryological approaches to insect segmentation. *Annu. Rev. Entomol.* **47**, 669-699.

Dearden, P. K. and Akam, M. (2001). Early embryo patterning in the grasshopper, Schistocerca gregaria: wingless, decapentaplegic and caudal expression. *Development* **128**, 3435-3444.

Hauptmann, G. and Gerster, T. (2000). Multicolor whole-mount in situ hybridization. *Methods Mol. Biol.* **137**, 139-148.

Hughes, C. L. and Kaufman, T. C. (2000). RNAi analysis of Deformed, proboscipedia and Sex combs reduced in the milkweed bug Oncopeltus fasciatus: novel roles for Hox genes in the Hemipteran head. *Development* **127**, 3683-3694.

Hughes, C. L. and Kaufman, T. C. (2002). Exploring myriapod segmentation: the expression patterns of even-skipped, engrailed, and wingless in a centipede. *Dev. Biol.* **247**, 47-61.

Hülskamp, M., Lukowitz, W., Beermann, A., Glaser, G. and Tautz, D. (1994). Differential regulation of target genes by different alleles of the segmentation gene hunchback in Drosophila. *Genetics* **138**, 125-134.

Isshiki, T., Pearson, B., Holbrook, S. and Doe, C. Q. (2001). Drosophila neuroblasts sequentially express transcription factors which specify the temporal identity of their neuronal progeny. *Cell* **106**, 511-521.

Jürgens, G., Wieschaus, E., Nüsslein-Volhard, C. and Kluding, H. (1984). Mutations affecting the pattern of the larval cuticle in *Drosophila melanogaster*. *Roux's Arch. Dev. Biol.* **193**, 283-295.

Krause, G. (1939). Die Eitypen der Insekten. *Biol. Zentralbl.* **59**, 495-536.

Lehmann, R. and Nüsslein-Volhard, C. (1987). hunchback, a gene required for segmentation of an anterior and posterior region of the Drosophila embryo. *Dev. Biol.* **119**, 402-417.

Lohs-Schardin, M., Cremer, C. and Nüsslein-Volhard, C. (1979). A fate map for the larval epidermis of Drosophila melanogaster: localized cuticle defects following irradiation of the blastoderm with an ultraviolet laser microbeam. *Dev. Biol.* **73**, 239-255.

Mellanby, H. (1935). The early embryological development of Rhodnius prolixus. *Q. J. Microsc. Sci.* **78**, 71-90.

O'Neill, J. W. and Bier, E. (1994). Double-label in situ hybridization using biotin and digoxigenin-tagged RNA probes. *Biotechniques* **17**, 870, 874-875.

Patel, N. H., Martin-Blanco, E., Coleman, K. G., Poole, S. J., Ellis, M. C., Kornberg, T. B. and Goodman, C. S. (1989). Expression of engrailed proteins in arthropods, annelids, and chordates. *Cell* **58**, 955-968.

Patel, N. H., Condron, B. G. and Zinn, K. (1994). Pair-rule expression patterns of even-skipped are found in both short- and long-germ beetles. *Nature* **367**, 429-434.

Patel, N. H., Hayward, D. C., Lall, S., Pirkl, N. R., DiPietro, D. and Ball, E. E. (2001). Grasshopper hunchback expression reveals conserved and novel aspects of axis formation and segmentation. *Development* **128**, 3459-3472.

Peterson, M. D., Popadic, A. and Kaufman, T. C. (1998). The expression of two engrailed-related genes in an apterygote insect and a phylogenetic analysis of insect engrailed-related genes. *Dev. Genes Evol.* **208**, 547-557.

Robb, J. A. (1969). Maintenance of imaginal discs of Drosophila melanogaster in chemically defined media. *J. Cell Biol.* **41**, 876-885.

Rogers, B. T. and Kaufman, T. C. (1996). Structure of the insect head as revealed by the EN protein pattern in developing embryos. *Development* **122**, 3419-3432.

Sander, K. (1976). Morphogenetic movements in insect embryogenesis. In *Insect Development* (ed. P. A. Lawrence), pp. 35-52. Oxford: Blackwell.

Sander, K., Gutzeit, H. and Jäckle, H. (1985). Insect embryogenesis: morphology, physiology, genetical and molecular aspects. In *Comprehensive Insect Physiology Biochemistry and Pharmacology*, Vol. 1 (ed. G. A. Kerkut and L. I. Gilbert), pp. 319-385. Oxford: Pergamon Press.

Schröder, R. (2003). The genes *orthodenticle* and *hunchback* substitute for bicoid in the beetle *Tribolium*. *Nature* **422**, 621-625.

Sommer, R. and Tautz, D. (1991). Segmentation gene expression in the housefly Musca domestica. *Development* **113**, 419-430.

Spradling, A. C. and Rubin, G. M. (1982). Transposition of cloned P elements into Drosophila germ line chromosomes. *Science* **218**, 341-347.

St Johnston, D. and Nüsslein-Volhard, C. (1992). The origin of pattern and polarity in the Drosophila embryo. *Cell* **68**, 201-219.

Tautz, D., Lehmann, R., Schnürch, H., Schuh, R., Seifert, E., Kienlin, A., Jones, K. and Jäckle, H. (1987). Finger protein of novel structure encoded by *hunchback*, a second member of the gap class of *Drosophila* segmentation genes. *Nature* **327**, 383-389.

Telford, M. J. and Thomas, R. H. (1998). Expression of homeobox genes shows chelicerate arthropods retain their deutocerebral segment. *Proc. Natl. Acad. Sci. USA* **95**, 10671-10675.

Wolff, C., Sommer, R., Schröder, R., Glaser, G. and Tautz, D. (1995). Conserved and divergent expression aspects of the Drosophila segmentation gene hunchback in the short germ band embryo of the flour beetle Tribolium. *Development* **121**, 4227-4236.